THE EFFECTS OF PLANET SCATTERING ON PLANETARY SYSTEM ARCHITECTURE

By

TREVOR JAMES SMITH

_____

A Thesis Submitted to The Honors College

In Partial Fulfillment of the Bachelors degree
With Honors in

Astronomy

THE UNIVERSITY OF ARIZONA

M A Y 2 0 2 0

Approved by:

_____

Dr. Kaitlin Kratter
Department of Astronomy

The Effects of Planet Scattering on Planetary System Architecture

Trevor J. Smith[1]

[1]*Steward Observatory*
933 North Cherry Avenue
Tucson, AZ 85721-0065

(Dated: May 13, 2020)

ABSTRACT

In contrast to idealized planet systems of uniform masses and separations, more complex systems informed by observations of multiple-exoplanet systems are not as well understood. To better understand observed exoplanet systems, recent studies have focused on the more complex interactions between planets of unequal masses. In this study, we seek a broad understanding of dynamical evolution in planet populations with qualitatively different mass distributions, starting from compact multiple-planet systems. We find that for all populations, the progression from compact to loosely spaced planets is driven by planet scattering events, which disrupt planets pairs with low dynamical spacing. Our results suggest that the final average dynamical spacing that a population evolves to is correlated with the ratio of high to low mass planets. We also suggest that low numbers of high mass planets disproportionately drive planet losses due to ejections, as we see the dominance of collisions between planets only when the mass distribution is truncated before the high mass regime.

1. INTRODUCTION

Computational N-body simulations have been an indispensable tool in the study of planetary dynamics. Stars with multiple planets are inherently chaotic systems, making any predictions uncertain over a long enough period of time. Even the Solar System, which has been in the same stable configuration for $> 4\,\mathrm{Gyr}$, has been numerically shown to undergo dynamic instability on long enough timescales (e.g., Laskar 1989). We define dynamic stability as the certainty that planets will not undergo close approaches with each other, such that the force of gravity between them never dominates over that of the star. These close approaches are also referred to as planet scattering events, and they can have dramatic consequences for the overall architecture of a planetary system. Due to the tremendous accelerations planets can exert on each other at close proximity, their orbits can be significantly altered or their order in the system rearranged.

It has been shown that for a two planet system, dynamic stability can be proven under specific circumstances. Two planets of masses m_1 and m_2, on initially circular orbits around a central star with mass $M_* \gg m_1 + m_2$, will be dynamically stable if the difference between their semimajor axes is above a certain threshold: $a_2 - a_1 > 2\sqrt{3}R_{H,m}$ (Gladman 1993). Here a_2 and a_1 are the semimajor axes of the exterior

and interior planets, respectively, and $R_{H,m}$ is their mutual Hill radius:

$$R_{H,m} = \left(\frac{m_1 + m_2}{3M_*}\right)^{\frac{1}{3}} \frac{a_1 + a_2}{2} \tag{1}$$

Unfortunately, for any other situation than this idealized two planet system, dynamical stability for all time cannot be proven. Despite this, using units of $R_{H,m}$ to describe the separation of the planets is common in studies on planet dynamics. From this we define a dimensionless parameter for the separation between planets, often called the dynamical spacing:

$$\beta = \frac{a_2 - a_1}{R_{H,m}} \tag{2}$$

There have been a number of studies that explore how β influences stability in systems of more than two planets. Since dynamical stability cannot be proven in these systems for all time, often the stability timescale is measured: the time elapsed until first instability. Starting from systems of planets with very uniform masses and dynamical spacings, Chambers et al. (1996) explores the effects of β, planet multiplicity (number of planets), and μ (m_{planet}/M_*) on the stability timescale. Studies such as this, working with very uniform and ideal systems, are very informative to our sense of what affects dynamic stability.

The past two decades have proven to be the era of exoplanet discovery, as the number of known exoplanets has grown from a handful to the thousands discovered over the *Kepler* space telescope's lifetime. In this period, N-body simulations received a new utility and mission: explore the role of planet dynamics in observed systems. Simulations have proven to be useful in following up observations by confirming the stability of multiple-planet systems (Lissauer et al. 2011). Gravitational interactions between planets seem to influence the architecture of real life systems, as the stability many observed multiple-planet systems is precarious (Pu & Wu 2015). In addition to assessing the stability of multiple-planet systems, simulations can be used to analyze the nature and results of the instability. For example, some studies have sought to test planet formation theories by comparing the dynamically evolved theoretical systems with the observed properties of exoplanet systems (Jurić & Tremaine 2008; Chatterjee et al. 2008).

The mission of understanding the dynamics of real exoplanet systems have made it necessary to understand the dynamics of diverse planetary systems. The true mass distribution of planets in the galaxy is not known due to observational biases that prevent us from obtaining complete information on any planetary system save the Solar System. In our Solar System we observe small terrestrial planets coexisting with gas giants, and some estimations suggest that this is not uncharacteristic (Malhotra 2015). There have been recent studies that suggest more diverse planet systems, especially in terms of mass, have qualitatively different dynamics than homogeneous

ones. Morrison & Kratter (2016) show that the relationship between β and stability timescale becomes more complicated for very high planet masses due to the increasing importance of higher order mean motion resonances. The interactions between unequal mass planets can also be complex. There is evidence to suggest that the presence of one massive planet at a large semimajor axis can affect the interactions of less massive planets in closer orbits, resulting in tighter packed systems than otherwise predicted (Hands & Alexander 2016).

As discussed above, in order to better understand the dynamics of real planetary systems, future studies must further explore the process of dynamical instability and what it leaves behind, as well as the interactions between very unequal mass planets. It is our goal in this study to compare and contrast the effects of dynamical evolution on planet populations with qualitatively different mass distributions. We wish to understand broadly how planet scattering events sculpt planet populations in initially compact configurations.

2. METHODS

2.1. *Measures of Planet-Planet Interaction*

Much of our analysis in this study is focused on the dynamics of adjacent planet pairs. We use the term adjacency in the sense of ordering the planets by their semimajor axis. Adjacency between any particular pair of planets are not necessarily conserved in these simulations due to planet scattering events. For example, the order of two planets could switch or two new planets become adjacent when the planet in between is removed from the system.

We considered two parameters to measure the interaction between two planets. The first is the dynamical planet spacing β (Eq. 2), also known as the planet spacing in units of mutual Hill radii (Eq. 1). Our motivations in choosing this parameter are twofold. First, as mentioned in Section 1, planet spacing measured in these units are historically relevant due their use in the stability criterion in the three-body problem Gladman (1993). Second, despite this stability criterion being invalid for systems of three or more planets, the parameter is still useful as a rough estimate for the strength of planet-planet interactions and the likelihood of a planet scattering event.

The second parameter of planet-planet interaction is the period ratio, $\mathcal{P}$. Under the assumption of Keplerian orbits, and that $m_{Planet} \ll M_*$, we calculated $\mathcal{P}$ as the ratio of semimajor axes to the three-halves power:

$$\mathcal{P} = \left(\frac{a_2}{a_1}\right)^{\frac{3}{2}} \tag{3}$$

where a_1 and a_2 are the semimajor axes of the interior and exterior planets, respectively. By our definition, $\mathcal{P}$ is always ≥ 1. $\mathcal{P}$ does not capture any information about the masses of either of the planets, so a particular value for period ratio could be relatively stable for two low-mass planets while being highly unstable in the presence

of a high-mass planet. Despite this, $\mathcal{P}$ remains a good estimate of how often two planets interact.

When analyzing $\mathcal{P}$ in this study, we do not report information on mean motion resonances for two reasons. First, we do not predict mean motion resonances to be important in our constructed planetary systems. Our systems start out relatively compact, in the regime where planet scattering and more proximity-sensitive interactions dominate. Second, mean motion resonances are quite rare in pure gravitational N-body simulations like ours, which lack any dissipating forces.

2.2. *Simulations*

Our data comes from the gravitational N-body simulations conducted and reported in Smullen et al. (2016). The full data set of this study includes both single star planetary systems as well as circumbinary ones, however, the subset of single star planet systems is sufficient for our purposes. From this, our data set consists of 400 runs, in which a single planetary system is simulated for 10 million years. Each run begins with 10 planets whose properties, such as mass and orbital parameters, were randomly drawn from statistical distributions described in section 2.3. The integration was computed using a Guass-Radau scheme from the Mercury software package (Chambers & Migliorini 1997). This is an adaptive time-step, non-symplectic integrator, which was necessary to accurately resolve the chaotic close encounters between planets as well as the slow secular evolution between these encounters (Smullen et al. 2016).

Collisions between any two bodies and ejections from the system were all included in the simulations to properly capture the results of planet scattering events.

Planet-planet collisions were decided when the planets came within a distance equal to the sum of their radii. Planet radii were calculated from the randomly drawn mass parameter (discussed in section 2.3) and the assumption of a constant density $\rho = 1$ g cm^{-3}. When a collision between planets is detected, the two planets are merged into one while conserving both mass and momentum.

Planet-star collisions were calculated in the same manner, where the stellar radii were calculated from the mass-radius relationship in Demircan & Kahraman (1991). Mass and momentum are again conserved in the parameters of the star after the planet is removed.

Planet ejections, in which a planet becomes gravitationally unbound from the star, were handled simply by removing any planet that moves beyond a radius of 1000 AU from the central body.

2.3. *Initial Planetary Systems*

To initially populate each simulation run with planets, 10 planets were chosen with parameters randomly drawn from theoretical planet populations and placed in orbit around a one solar mass star. Four populations were defined and used for 100 runs

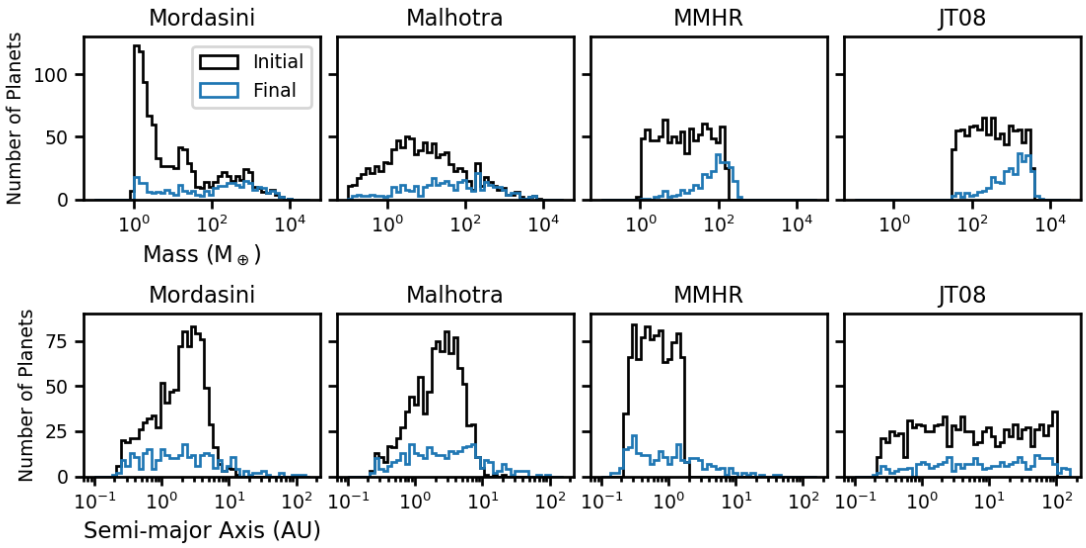

Figure 1. Histograms showing mass and semimajor axis distributions for each of the four planet populations. Each column displays information for one of the populations. The black histogram lines demonstrate the initial distributions, while the blue ones indicate the distributions at 10 million years.

each. In this section, we will summarize these planet populations from Smullen et al. (2016).

The inclination and eccentricity distributions of all planet populations were chosen to be Rayleigh distributions, with scale factors of $e = 0.1$ and $i = 5.73°$ following the models of Jurić & Tremaine (2008). The mass and semimajor axis distributions for each population were chosen to match either a theoretical or observationally-motivated model of planet formation. These distributions, and how they appear at 10 Myr are shown in Figure 1. Below we discuss the details of how these planet populations were initialized.

Mordasini. This planet population was modelled after the planet synthesis model of Mordasini et al. (2009a) and Mordasini et al. (2009b). These papers present a two-dimensional theoretical distribution of a semimajor axes and masses for planets. For these simulations, two separate one-dimensional distributions for these parameters were deconstructed from this and independently sampled. The resulting distribution of semimajor axes ranges from 0.1 to 15 AU with a peak at 3 AU. The distribution of masses range from 1-$10^4 M_\oplus$, with a large peak at low masses and two less prominent peaks at Neptune and Jupiter masses.

Malhotra. This population follows the analysis presented in Malhotra (2015), in which the real mass distribution of planets was estimated from the observed distributions of $\mathcal{P}$ and β in *Kepler* multiple-planet systems. This mass distribution was modeled as log-normal, where $\log(m/M_\oplus)$ has $\mu = 0.8$ and $\sigma = 1.15$. The semimajor axis distribution for our planet population was derived from this model, which produced a gamma distribution starting from 0.1 AU and tapering off at approximately 32 AU.

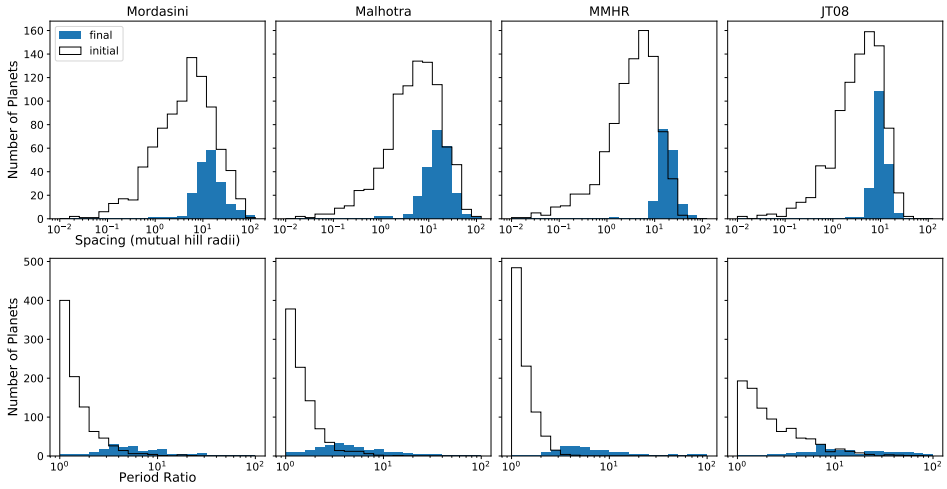

Figure 2. Histograms showing the dynamical spacing (top row) and period ratio (bottom row) between adjacent planet pairs in each of our planet populations (separated by columns). Initial values, for planet pairs present at the beginning of the simulation, are shown by the black line histograms. These are overlaid onto the final values for adjacent planet pairs present at 10 Myr, shown by the solid blue histograms.

JT08. This population is directly modeled in the 'c10s10' ensemble presented in Jurić & Tremaine (2008). The distribution of semimajor axes is log uniform in the range from 0.1 to 100 AU. Masses are also drawn from a log uniform distribution between 0.1 and 10 M_J.

MMHR. This planet population, which stands for Matched Mutual Hill Radius, was modeled in Smullen et al. (2016) as a more compact analog to JT08. Both semimajor axis and mass are again log uniform, ranging from 0.1 to 1.7 AU and 1 to 160 $M_\oplus$ respectively. The resulting distribution of dynamical planet spacings (eq. 2) should exactly match that of JT08. However, with scaled down planet masses, this results in very compact systems.

3. RESULTS

3.1. *Dynamics of Adjacent Planet Pairs*

In compact planetary systems such as these, we predict the dominant form of planet-planet interactions to be close-proximity interactions between adjacent planets. As discussed in Section 2.1, we chose the dynamical planet spacing β and period ratio $\mathcal{P}$ as parameters to measure the dynamics of these adjacent pairs. In Figure 2 we report our calculations of β and $\mathcal{P}$ for adjacent planet pairs within each population. We also compare the measurements taken at the beginning (T=0) and end (T=10 Myr) of the simulations.

In our initial measurements for $\mathcal{P}$ (Figure 2), we find the distribution to be significantly peaked near 1, the smallest value possible. Since $\mathcal{P}$—which depends only on semimajor axes—is a measure of the real spacing between planets, this is a result of

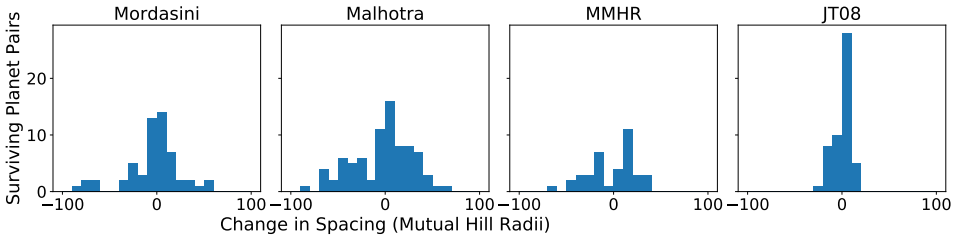

Figure 3. Histograms showing the change in dynamical spacing ($\Delta\beta$) for surviving planet pairs only. We define surviving planet pairs as adjacent planet pairs at 10 Myr which were also adjacent, without changing order, at the beginning of the simulation. In units of mutual Hill radii, positive data indicate further spaced pairs, negative show compacted pairs. Pairs with values near 0 show a similar spacing at 10 Myr compared to their starting conditions.

the initially tightly packed architecture of these systems. The distributions have positive tails of varying lengths, with JT08 having the most extended tail to $\mathcal{P} = 20$ and MMHR being truncated to within 5. This correctly reflects these two distributions as being the initially most compact and extended populations in semimajor-axis. By 10 Myr in every population, the low peaks are completely depleted and the distribution of $\mathcal{P}$ becomes very spread out along a wide range, with MMHR and JT08 both showing measurements near 100. Every distribution shows an evolution from an initially very compact state to a more widely spaced one.

The distributions for β (Figure 2) also show the general progression from compactness to wider spread in the $R_{H,m}$ parameter space. Unlike $\mathcal{P}$ however, the final β distributions appear to have completely evacuated the lower end of their initial distributions (below 1 mutual Hill radius), while remaining approximately within the range of their initial distribution. We note that the appearance of the final distributions being more tightly spread in Figure 2 is a result of the logarithmic scale. JT08 is the only population for which the standard deviation of β does decrease.

3.2. *Surviving Planet Pairs*

In Figure 2, the final histograms for β within each population, with the exception of MMHR, seem to be completely contained within the initial ones. Moreover, the final histograms seem to just fill out the positive slope of the initial ones. This suggests that, between initial and final measurements, low β measurements are depleted while high values for β remain unchanged. However, we cannot determine the causal connection between initial and final measurements from Figure 2 alone. It is also possible that a wide range of values for β are lost throughout the simulation, and the remaining distribution is shifted to the higher values.

Figure 3 is our attempt to illuminate this situation. Here we plot the change in β for surviving adjacent planet pairs only. We define this as an adjacent planet pair present at the end of the simulation, which was also adjacent and in the same order at the beginning. Despite the low number of pairs that meet this criteria in each population, Figure 3 shows $\Delta\beta$ to be peaked near 0 and more or less symmetric

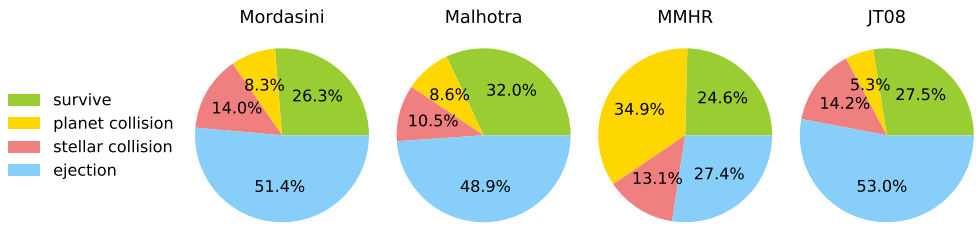

Figure 4. Pie charts indicating the proportions of different end statuses for planets at 10 Myr in each of the planet populations. Possible end statuses include ejected from the system, removed in a collision, or neither of these (planet survives to 10 Myr). Planets removed by collisions are further divided into planet-planet and planet-star collisions.

around this peak for every population except MMHR. This suggests that the mean β for surviving adjacent planet pairs does not change significantly from the initial to final state, and the shift seen in Figure 2 is not a result of this subset of planet pairs.

Figure 3 also shows that the behavior of surviving adjacent planet pairs is different in MMHR than in the other populations. We see no peak at $\Delta\beta = 0$, however further analysis of this irregular looking distribution is hindered by the lack of data. This could be the result of a lower planet survival rate in general (shown in Figure 4) and lack of planet pairs that meet our criteria for surviving with adjacency.

3.3. *Planet Loss Mechanisms*

To further illuminate the effects of planet scattering on the dynamics of adjacent planet pairs, here we discuss the proportions of planets removed from each population in planet scattering events. Figure 4 shows the survival rates of planet in each of the planet populations, as well as the rates at which planets are removed by different mechanisms of the simulation. These mechanisms (discussed in Section 2.2) include ejections and collisions, either with another planet or the central star. The two most similar planet populations in this respect are Mordasini and JT08, between which no category differs by more that 3% of the population. Malhotra is also reasonably similar to these two, with a higher survival rate by 4.5-6% and slightly lower ejection and stellar collision rates. The MMHR population differs significantly from the others. MMHR has 26.3% more of its planets removed by planet-planet collisions than any other population, and 21.5% fewer ejections as well.

3.4. *Statistical Distributions for Planet Spacing*

Our goals in this section are to report on the effects of planet scattering on β in a way that is useful to future studies and the development of models. We chose to fit log-normal probability density functions to our final distributions for β, shown in Figure 5. We felt that log-normal distributions fit the data reasonably well, with some caveats. First, our measured distributions have slightly higher peaks than captured by the best fit curves. Second, the curves do not reflect the small but significant collection of measurements around 1 mutual Hill radius. It is unclear if these negative outliers

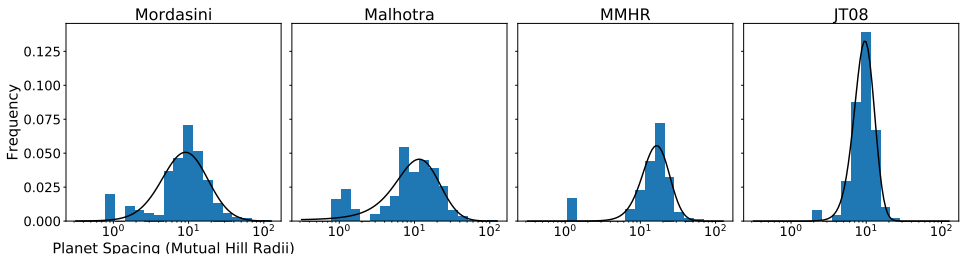

Figure 5. Normalized histograms for β in blue, with black lines indicating fitted log-normal probability density functions. Log-normal distributions fit reasonably well except in the following two areas. The PDF 1) underestimates the observed distribution very close to the peak and 2) does not account for the few pairs with extremely low spacing (near 1 MHR).

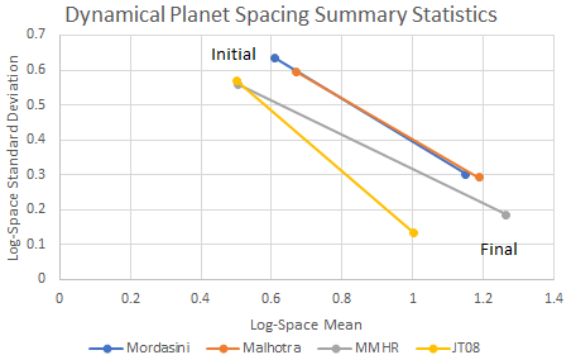

Figure 6. Summary statistics for $log(\beta)$ in each planet population. Mean is plotted on the horizontal axis and standard deviation on the vertical axis. Initial and final values for each population are connected by line segments. Under the assumption of a log-normal distribution in β, this plot shows the progression of fit parameters.

actually represent stable adjacent planet pairs. Further investigation into these erratic outliers may be worthwhile, as there are even within the analytic stability limit for an ideal two planet system (outlined in Section 1).

In Figure 6 we display how the distribution of $\log \beta$ for each population changes in mean and standard deviation. This presents the information in Figure 2 from a more quantitative perspective. If a log-normal distribution is assumed, this plot also describes the change in the fit parameters. JT08 and MMHR start out with nearly identical fit parameters, but at 10 Myr they are the most different in terms of their means. Mordasini and Malhotra on the other hand start and end close together, tracing out a similar path. These two populations at 10 Myr also have significantly higher standard devations for $\log \beta$ than MMHR or JT08.

4. DISCUSSION

4.1. *Dynamical Sculpting*

As discussed in Section 3.1, our measured distributions of the dynamical spacing, β, for each planet population at 10 Myr seem to fill out the high-value tails of their initial distributions while containing no data at the low-value tails (Figure 2). In

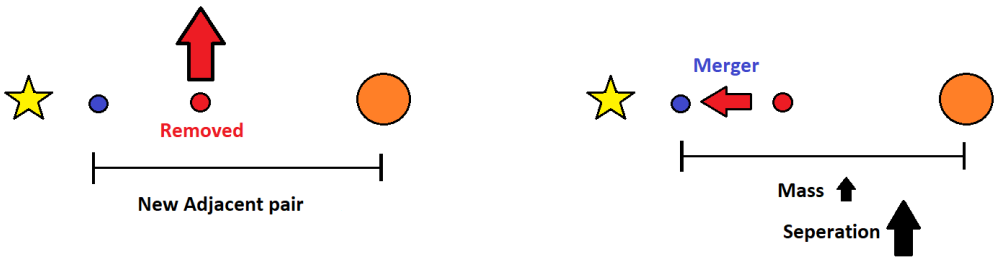

(a) (b)

Figure 7. Simple illustrations demonstrating two mechanisms of planet scattering that results in higher overall dynamical spacing. Figure (a) demonstrates the results of a clean ejection or stellar collision, where a partner in a low β pair is removed from the system with little effect on other planets. If the removed planet has two adjacent neighbors, then the resulting new adjacent pair will have a higher β. Figure (b) demonstrates a planet collision and merger. While the new adjacent pair has a higher mass, β is much more sensitive to changes in separation, so the resulting $\Delta\beta$ from this process is more likely to be positive.

Section 3.2 we reported on how β changes for surviving adjacent planet pairs, that is adjacent planet pairs present at 10 Myr that were also adjacent and in the same order at initialization. We concluded that the distribution of $\Delta\beta$ for these subsets of the population are approximately symmetric about $\Delta\beta = 0$ (Figure 3). Therefore, the positive shift in β distributions from initialization to 10 Myr is not a result of surviving adjacent planet pairs becoming on average more widely spaced.

With all else being equal, a higher β between two planets generally implies greater dynamic stability, meaning that planet scattering is less likely. This implies that the migration of our planet populations' β distributions can be thought of as overall evolution towards stability against planet scattering. But what drives this migration? Our evidence in the paragraph above indicates that this migration towards stability is not driven by planet pairs whose adjacency is conserved throughout the simulation. This implies that the evolution towards stability is the result of changes in the configuration of planetary systems, i.e. rearrangement in the order of planets or the removal of planets through collisions and ejections. In other words, unstable planet pairs don't become stable, they are disrupted by planet scattering events.

There are many ways in which planet scattering events result in a higher overall β. The simplest situation is that of a clean planet ejection or stellar collision. This is almost equivalent to one of the planets in a low β, unstable pair disappearing. If the remaining planet has a significantly higher mass, then the rest of the system is especially unaffected, as that planet would not lose too much of its own angular momentum during the scattering. A more complex interaction is a planet collision. There are two competing factors in the resulting values for β after a collision and merger. The first is that after two nearby planets become one, the real separation (Δa) with its new neighbors will be considerably higher. However, due to a higher

mass merger remnant, the units of beta ($R_{H,m}$, Eq. 1) will be larger. However, the new value for β is proportional to Δa and decreases with $\Delta m^{1/3}$, so nearly always the value is driven up. These two processes are illustrated in Figure 7. There are many more mechanisms by which planet scattering alters the resulting architecture of the system, but the overall trend is towards increasing β.

4.2. *Effect of Massive Planets*

In this section we compare and contrast the dynamical evolution of the JT08 and MMHR populations and discuss the effects of different planet mass distributions. As discussed in Section 2.3, MMHR was designed to reproduce the β distribution of JT08 with a lower range of planet masses. This makes comparing these two populations ideal for isolating the effects of planet masses. The Mordasini and Malhotra populations were constructed from much wider mass distributions, incorporating planets from both regimes. The consequences of a more diverse set of planet masses on dynamical evolution is also discussed in this section.

In Section 3.4 we discussed the evolution of the β distributions and found that MMHR and JT08, starting from nearly identical initial statistics, diverge significantly in their final statistics. MMHR has the highest mean β at 10 Myr of all the planet populations, while JT08 has the lowest (Figure 6). We find the most likely explanation of this divergence to be the mass dependence of stability predicted by β, mentioned in Section 1. In general, high mass planet pairs have a lower threshold than low mass pairs, in terms of β, to achieve a similar stability timescale. MMHR is composed of consistently lower mass planets than JT08, so overall stability over millions of years in MMHR would be reflected in a higher average β.

The Mordasini and Malhotra populations are composed of planets in both mass regimes, producing a wider variety of planet pair masses. Following the same line of reasoning above, we would predict the average β of these two populations at 10 Myr to be between the two extremes. Moreover, the larger spread of stability thresholds in β should be reflected by a larger spread in the β distribution. Both of these predictions are confirmed by the results presented in Section 3.4.

The MMHR and JT08 populations also differ dramatically in the mechanisms by which their planets are removed, outlined in Section 3.3. While both populations have similar survival rates, MMHR has many more planets removed in planet-planets collisions, and JT08 has many more ejections. It makes sense that the outcomes of planet scattering events do not depend on β. β is based on osculating orbital parameters, which are no longer valid during the major perturbation of a planet scattering event. While β can be interpreted as an estimate of the strength of gravitational interaction between two planets, its usefulness lies in determining the likelihood of a planet scattering event. The outcome of a scattering event depends on two factors: whether the planets collide, and if not, the momentum exchange that takes place. The likelihood of the former increases with decreasing volume, so planets within a smaller semima-

jor axis range are more likely to collide. Additionally, the latter depends on planet mass. Massive planets can give larger kicks to their scattering partner, increasing the likelihood of ejection. The MMHR population has much smaller semimajor axes and planet masses, so it is likely that both of these factors are driving the high planet collision rate that we observe.

The behavior of the Mordasini and Malhotra populations, in terms of their ejection and collision rates, is not the average of these two extremes. Despite the significant number of low mass planets in their populations, their behavior is remarkably similar to that of JT08. This seems to suggest that the presence of any massive planet can drive ejections. In terms of mass distributions, the long positive tails of the Mordasini and Malhotra populations likely disproportionately affect the loss mechanisms for planet scattering processes.

5. CONCLUSION

In this study, we analyzed the data set resulting from N-body planet scattering simulations conducted and reported in Smullen et al. (2016). Our goal was to gain a broad perspective on the overall dynamical evolution of planet populations consisting of many multiple-planet systems. We found that the progression of a planet population from compact to loosely spaced, as determined by the dynamical planet spacing β, is driven by the disruption of unstable planet pairs by rearrangement or the removal of a planet from the system. Adjacent planet pairs whose adjacency is conserved do not show a trend of becoming more widely spaced, on average.

Another goal of our analysis was to compare the effects of dynamical evolution on planet populations of qualitatively different mass distributions. We compared the changing statistics of four different planet populations, two with diverse mass distributions and two with more homogeneous ones. Of the two more uniform populations, one was made up of consistently high-mass planets while the other had a very low-mass makeup. We found that, following the different stability thresholds in β for different mass planets, the consistently low mass population evolved to a significantly higher average β than the high mass population. The populations of more diverse mass makeup evolved to an average β between these two extremes, but their spread was significantly higher. Additionally, our results regarding the planet loss mechanism in planet scattering events suggest that high mass tail of a mass distribution has a disproportionate influence on loss mechanisms. We found that all planet populations with any massive planets at all showed a similar high ejection to collision ratio. A mass distribution that is truncated before reaching the high-mass regime will drive down planet loss by ejection from the system and increase the likelihood of collisions between planets.

We sincerely thank Dr. Kaitlin Kratter and Rachel Smullen (University of Arizona) for their contributions and support in this project.

REFERENCES

Chambers, J. E., Wetherill, G. W., & Boss, A. P. 1996, Icarus, 119, 261, doi: 10.1006/icar.1996.0019

Chambers, J. E. E., & Migliorini, F. 1997, in AAS/Division for Planetary Sciences Meeting Abstracts #29

Chatterjee, S., Ford, E. B., Matsumura, S., & Rasio, F. A. 2008, The Astrophysical Journal, 686, 580, doi: 10.1086/590227

Demircan, O., & Kahraman, G. 1991, Astrophysics and Space Science, doi: 10.1007/BF00639097

Gladman, B. 1993, Icarus, doi: 10.1006/icar.1993.1169

Hands, T. O., & Alexander, R. D. 2016, Monthly Notices of the Royal Astronomical Society, 456, 4121, doi: 10.1093/mnras/stv2897

Jurić, M., & Tremaine, S. 2008, The Astrophysical Journal, 686, 603, doi: 10.1086/590047

Laskar, J. 1989, Nature, 338, 237, doi: 10.1038/338237a0

Lissauer, J. J., Ragozzine, D., Fabrycky, D. C., et al. 2011, Astrophysical Journal, Supplement Series, 197, doi: 10.1088/0067-0049/197/1/8

Malhotra, R. 2015, Astrophysical Journal, 808, doi: 10.1088/0004-637X/808/1/71

Mordasini, C., Alibert, Y., & Benz, W. 2009a, Extrasolar planet population synthesis: I. Method, formation tracks, and mass-distance distribution, doi: 10.1051/0004-6361/200810301

Mordasini, C., Alibert, Y., Benz, W., & Naef, D. 2009b, Astronomy and Astrophysics, doi: 10.1051/0004-6361/200810697

Morrison, S. J., & Kratter, K. M. 2016, The Astrophysical Journal, 823, 118, doi: 10.3847/0004-637x/823/2/118

Pu, B., & Wu, Y. 2015, Astrophysical Journal, 807, doi: 10.1088/0004-637X/807/1/44

Smullen, R. A., Kratter, K. M., & Shannon, A. 2016, Monthly Notices of the Royal Astronomical Society, 461, 1288, doi: 10.1093/mnras/stw1347